IEEE Access
Multidisciplinary | Rapid Review | Open Access Journal

Received November 15, 2018, accepted December 10, 2018, date of publication December 24, 2018,
date of current version January 16, 2019.

Digital Object Identifier 10.1109/ACCESS.2018.2889506

Nearest Centroid Neighbor Based Sparse Representation Classification for Finger Vein Recognition

SHAZEEDA SHAZEEDA AND BAKHTIAR AFFENDI ROSDI
School of Electrical and Electronic Engineering, Engineering Campus, Universiti Sains Malaysia, Nibong Tebal 14300, Malaysia
Corresponding author: Bakhtiar Affendi Rosdi (eebakhtiar@usm.my)

This work is supported by Universiti Sains Malaysia Bridging Fund No. 304/PELECT/6316089.

ABSTRACT In this paper, an efficient finger vein recognition algorithm based on the combination of the nearest centroid neighbor and sparse representation classification techniques (*k*NCN-SRC) is presented. The previously proposed recognition algorithms are mainly based on distance computation. In the proposed method, the distance, as well as the spatial distribution, are considered to achieve a better recognition rate. The proposed method consists of two stages: first, the *k* nearest neighbors of the test sample are selected based on the nearest centroid neighbor, and then, in the second stage, based on the selected number of closest nearest centroid neighbors (*k*), the test sample is classified by sparse representation. Findings from the proposed method *k*NCN-SRC demonstrated an increased recognition rate. This improvement can be attributed to the selection of the train samples, where the train samples are selected by considering the spatial and distance distribution. In addition, the complexity of SRC is reduced by reducing the number of train samples for the classification of the test sample by sparse representation and the processing speed of the proposed algorithm is significantly improved in comparison with the conventional SRC which is due to the reduced number of training samples. It can be concluded that the *k*NCN-SRC classification method is efficient for finger vein recognition. An increase in the recognition rate of *3.35%*, *9.07%*, *20.23%*, and *0.81%* is obtained for the proposed *k*NCN-SRC method in comparison with the conventional SRC for the four tested public finger vein databases.

INDEX TERMS Distance criterion, finger vein recognition, *k*-nearest centroid neighbor, sparse representation classification, spatial distribution.

I. INTRODUCTION

Finger vein recognition is one of the hot topics in recent years in biometric research. Finger vein is a hypodermic recognition pattern of blood vessels which is unique for each individual, including identical twins, and the pattern for each finger is different within the same individual [1]. Amidst the diverse characteristics of biometrics such as commonality, uniqueness, and consistency, finger vein recognition exhibits some good advantages over the other biometric characteristics [2], [3] such as:

- Resist faking: As the finger vein is embedded inside the skin it resists manipulation, and hence it is difficult to be forged.
- Aliveness check: The finger vein recognition system works based on aliveness detection, as the finger vein image can only be accessed for a live person and hence it cannot be faked.
- User-friendly: As capturing of the finger vein image is contactless, it prevents the user from contamination and other displeasing effects. Hence it is user-friendly.

So far few methods have been reported for utilization in finger vein recognition, and most of them have focused on feature extraction. Among them, extraction of the finger vein using curvature in radon transform which detects the valley like structures [4], representation of features of the finger vein based on adaptive vector field estimation [5], affine invariant feature matching [6], Direction Variance Boundary Constraint Search (DVBCS) [7] to restore broken finger-vein patterns, vein extraction by structure analysis algorithm [8], the fusion of multi-scale matched filtering, and line tracking techniques [9] have been reported. Apart from feature extraction methods for finger vein recognition, some research work has also been proposed based on different classification techniques. The classification of finger vein images by

Support Vector Machine (SVM) is based on the separation of training samples by a hyperplane [10]. The larger the distance to the nearest training sample of any class the better the separation achieved. The SVM method has difficulty in kernel selection for setting the parameters properly for optimal results of classification in order to generate the model from the training data. Another classification technique for finger vein recognition is by Sparse Representation Classifier (SRC) [11]. In this approach, the finger vein images are represented sparsely and create a dictionary matrix of training samples. This dictionary matrix then represents the test sample. It is a computationally complex and time-consuming classification technique. Recently, another classification method for finger vein recognition was reported, called Fuzzy based k Nearest Centroid Neighbor (FkNCN) [12]. This method is based on nearest centroid neighbor, and then the fuzzy membership function is used to assign the class for the test sample.

Despite certain limitations, SRC's popularity remains undiminished. Sparse Representation Classification is one of the most recent classifiers that have been proposed in all biometric systems such as face [13], iris [14], fingerprint [15], palm print [16], gait [17] and also finger vein [11]. The main aim of SRC is to represent the sample images using the dictionary of fundamental signals called atoms, which is the sparse representation for the image samples, and later the test sample is represented by the atoms of the dictionary matrix [11]. The sparse solution for the linear combination can be obtained by the L_1 norm optimization technique [18]. Obtaining the sparse solution is an iterative process and requires complex matrix operation which is computationally a very complex and time-consuming process. The dictionary of atoms obtained consists of variable properties in comparison to the actual transformation due to the problems inherent in image processing which may affect the recognition rate [19].

In order to reduce the complexity and processing time of SRC, a few methods have been proposed [20]–[23]. Zhang and Yang [20] proposed a k Nearest Neighbor based Sparse Representation Classification (kNN-SRC) method to overcome the problems of classification by sparse representation combining two classifiers, k-NN, and SRC. This method consists of two stages. In the first stage the train samples are selected by the Nearest Neighbor classification technique for the test sample and in the second stage, the test sample is classified by SRC using the selected train samples. Comparatively, the selected numbers of training samples are less, due to which the processing time is reduced. In the kNN-SRC [37] method, the selection of training samples is by applying only the distance criterion, whereas in the proposed kNCN-SRC method the selection is based on both the distance and symmetric criteria. Xu *et al.* [21] proposed a Two-Phase Test Sample Sparse Representation (TPTSR) method for face recognition in which the samples are represented sparsely in two stages. The k train samples for the test sample is obtained from all the training samples by sparse representation, and in the second phase, the classification of the test sample is obtained by linear combination of the selected number of previously computed k train samples from the first stage. In addition, Xu *et al.* [22] proposed another methodology called Coarse to Fine Face Recognition based on Sparse Representation (CFFR), in which the test sample is classified from a coarse to fine SRC technique. This method also comprises two stages. The first stage performs the sparse representation over all the training samples, and in the next stage, the weighted sum of the selected classes of train samples that are near to the test sample is determined. The basic strategy of this method is to remove the training samples, which are far from the test sample, and reduce the number of training samples for the second stage of classification. As the realization of the linear combination is computationally a complex process, applying it in two stages increases the complexity as well as processing time. Hence, for a large number of databases, the processing time is very high. Recently, Zeng *et al.* [23] proposed a Kernel Coarse to Fine Recognition (KCFR) based sparse representation method for face images. This method also consists of two stages, in the first stage the selection of the candidate classes is made based on feature space selection by the kernel function, and in the second stage the test sample is classified to a class from the candidate classes by sparse representation classification. However, the complexity of kernel function increases with a large number of training samples.

Except for the distance criterion, no other criteria are applied in the mentioned methodologies [20]–[23] for the first stage. The recognition is based on the minimum distance between the test sample and the train samples. Apart from the distance criterion, there is also another criterion that will affect the classification accuracy such as the symmetry criterion. The literal meaning of the symmetric distribution of an image is the distribution over the mean of the pattern. The k Nearest Centroid neighbors classification (k-NCN) [24] is based on both the distance and symmetric distribution of the samples. The overall idea of k-NCN is to find the nearest neighbor to the test sample, and also with the consideration that the nearest centroid neighbor is geometrically distributed over the query pattern evenly as possible. In SRC, the classification of the patterns is based on the distance factor (residual distances,) and there is no consideration of symmetric criteria [11]. The classification by SVM is achieved by considering the separation of the training samples over a hyperplane. The higher gap over the plane separates the correct from the incorrect training samples; however, the symmetric criterion is not a factor for classification [10]. The concept of k-NN classification is on the basis of the minimum distance between the train and the test samples only, without the symmetric criterion [12]. From the previous studies, it is observed that the SRC gives a higher recognition rate; hence motivated by the concept of k-NCN and SRC, a combination of k-NCN with SRC is proposed to solve the problems of the methods such as kNN-SRC, TPTSR, CFFR and KCFR methods mentioned earlier.

The proposed work in this paper is performed in two stages, where the nearest centroid neighbor classifier (NCN) is combined with sparse representation classifier (kNCN-SRC). In the first stage, the k train samples which are nearest to the test sample are selected based on the NCN classification. By applying the Euclidean distance calculation method, the distances between the training samples and test sample are computed. In the second stage, the selected k number of train samples are used to classify the test sample based on SRC. NCN consists of both distance and symmetric constraints which selects the best candidates for SRC and eliminates the far samples, thereby reducing the number of train samples for SRC. These factors will result in a higher recognition rate and faster processing speed.

As mentioned earlier, SRC is computationally a complex and time-consuming process. In the kNCN-SRC method, instead of considering all the train samples to be represented sparsely, in the second stage, only a few of the closest centroid neighbors are considered, thereby reducing the complexity and time of the SRC method. In kNN-SRC, the best candidates for the second stage are selected by the NN which is based only on the distance criterion. Similarly, in TPTSR and CFFR techniques, in the first stage, the best candidates are obtained by sparse classification which is also only based on the distance factor (residual values). Also in the KCFR method, in the first stage, the candidate classes are learned in the feature space selected by the kernel function. The selection of the classes is by the minimum residual value which is also based on distance factor.

In comparison to the actual transformation, the sparse solution obtained for an image in SRC consists of variable properties inherited from the image processing such as noise [19], which results in a lower recognition rate. Also, the complexity in obtaining the sparse solution increases the processing time. However, in the proposed kNCN-SRC method, the selection of the best candidates is by centroid distances which incorporates both the distance and symmetric criteria, resulting in a higher recognition rate than the conventional SRC. The selection of best candidates reduces the number of train samples for SRC classification which results in the fast processing speed.

The rest of this paper is organized as follows. Section II reviews the typical k-NCN, and SRC algorithms. Section III explains the proposed kNCN-SRC algorithm and also discusses the differences between the proposed method and the previously proposed methods. Section IV presents the experimental results of the proposed algorithm on four different finger vein data sets. Finally, in Section V the paper is concluded.

II. k-NCN AND SRC

A. k-NEAREST CENTROID NEIGHBOR (k-NCN)

NCN is an enhanced version of NN classification. The basic concept of NCN is to find the nearest neighbor for the given test sample based on the centroid (mean) point. The nearest centroid neighbor is similar to NN except that along with the proximity, the symmetric distribution is also accounted for [24]. Consequently, for the given test sample $\boldsymbol{y}$, the NCN algorithm is liable to the following compulsions [25]:

- The distance criterion: The centroid neighbors must be close to the test sample $\boldsymbol{y}$.
- The symmetric criterion: The centroid neighbors must be spatially distributed over the test sample $\boldsymbol{y}$, as closely as possible.

Mathematically, the NCN concept can be explained as follows. For the given set of training images $\boldsymbol{X}= \{ \boldsymbol{X}_1, \boldsymbol{X}_2, \ldots, \boldsymbol{X}_i, \ldots, \boldsymbol{X}_C\}$ with C classes, and $\boldsymbol{X}_i = \{ \boldsymbol{x}_1, \boldsymbol{x}_2, \ldots, \boldsymbol{x}_j, \ldots, \boldsymbol{x}_n\}$ where $\boldsymbol{X}_i \in R^{(m\times n)}$ has n number of images in the i^{th} class. Each image is assumed to be of dimension $m = p \times q$. The centroid for the set of points of class $\boldsymbol{X}_i$ can be computed as in (1).

$$x_n^C = \frac{1}{n}\sum_{j=1}^{n} \boldsymbol{x}_j \tag{1}$$

In this paper, the training and the test images are normalized to unit L_2 norm. The normalization is done to transform the features of the images to range from *0* to *1*. The k Nearest Centroid neighbors (k-NCN) for the given test sample $\boldsymbol{y}$ can be obtained by Algorithm 1(a) [26], [27].

Algorithm 1(a).

1) The first nearest centroid neighbor $\boldsymbol{T}_1^{NCN}$ is selected based on the minimum distance between the test sample $\boldsymbol{y}$ and all the train samples. This distance can be computed by Euclidean distance as in (2).

$$d(\boldsymbol{y}, \boldsymbol{x}_j) = \sqrt{(\boldsymbol{y} - \boldsymbol{x}_j)^T(\boldsymbol{y} - \boldsymbol{x}_j)} \tag{2}$$

2) The i^{th} nearest centroid neighbor, $\boldsymbol{T}_i^{NCN} (2 \le i \le k)$ is selected such that the present and the previously selected nearest centroid neighbors, i.e., $\{ \boldsymbol{T}_1^{NCN}, \boldsymbol{T}_2^{NCN}, \ldots, \boldsymbol{T}_{i-1}^{NCN}\}$ are as close to $\boldsymbol{y}$ as possible. The i^{th} centroid is given as the sum of the new point in $\boldsymbol{X}_i$ and all the previous centroid neighbors $\{\boldsymbol{T}_1^{NCN}, \boldsymbol{T}_2^{NCN}, \ldots, \boldsymbol{T}_{i-1}^{NCN}\}$ divided by i. The distance between the test sample $\boldsymbol{y}$ and the i^{th} centroid point is given by (3).

$$d(\boldsymbol{y}, \boldsymbol{x}_i) = \sqrt{(\boldsymbol{y} - \boldsymbol{x}_i^c)^T(\boldsymbol{y} - \boldsymbol{x}_i^c)} \tag{3}$$

where $\boldsymbol{x}_i^c$ is the i^{th} centroid point.

3) The i^{th} nearest centroid neighbor $\boldsymbol{T}_i^{NCN}$ is decided by the shortest distance computed by (3).
4) Steps 2 and 3 are repeated until i is equal to k

Consequently, the k-NCN classification concept can be applied in pattern recognition as follows.

Algorithm 1(b).

1) The k nearest centroid neighbors for the test sample $\boldsymbol{y}$ are determined by algorithm 1(a) as $\boldsymbol{G}_k^{NCN}(\boldsymbol{y}) = \{ \boldsymbol{T}_1^{NCN}, \boldsymbol{T}_2^{NCN}, \ldots, \boldsymbol{T}_i^{NCN}, \ldots, \boldsymbol{T}_k^{NCN}\}$.
2) The test sample $\boldsymbol{y}$ is assigned to the class C with the maximum number of votes from the set $\boldsymbol{G}_k^{NCN}(\boldsymbol{y})$.

(resolve ties randomly)

$$C = \arg\max_{C_i} \sum_{i=1(\boldsymbol{T}_i^{NCN} \in \boldsymbol{G}_k^{NCN}(\boldsymbol{y}))}^{k} \delta(C_i = Y_i^{NCN}) \quad (4)$$

where the class of i^{th} nearest centroid neighbor ($\boldsymbol{T}_i^{NCN}$) is Y_i^{NCN} and $\delta(C_i = Y_i^{NCN})$ is the kronecker delta function with the assumptions as *1* for $C_i = Y_i^{NCN}$ when the test sample is correctly classified and *0* for $C_i \neq Y_i^{NCN}$ when the test sample is wrongly classified.

B. SPARSE REPRESENTATION CLASSIFICATION (SRC)

In recent years, SRC has gained much importance in the field of pattern recognition. A finger vein recognition technique using the SRC algorithm was proposed by Xin *et al.* [11]. In this section, a brief review of the concept of SRC is explained. Sparse representation is a technique of representation of the image from the linear combination of atoms from a dictionary matrix. The test image is represented with respect to the atoms of the dictionary matrix, called the sparse coefficients.

Assume that there are C classes in the given train set $\boldsymbol{X} = \{\boldsymbol{X}_1, \boldsymbol{X}_2, \ldots, \boldsymbol{X}_i, \ldots, \boldsymbol{X}_C\}$. Each class consists of n number of images with the dimension of $m = p \times q$. Let $\boldsymbol{X}_i = \{\boldsymbol{x}_1, \boldsymbol{x}_2, \ldots, \boldsymbol{x}_n\}$, where $\boldsymbol{X}_i \in R^{(m \times n)}$, be the n number of training images in the i^{th} class. A test image $\boldsymbol{y}$ from an unidentified class can be represented by the linear combination of the train set as,

$$\boldsymbol{y} \approx \boldsymbol{X}\boldsymbol{\alpha} \quad (5)$$

where $\boldsymbol{\alpha} = \{\boldsymbol{\alpha}_1, \boldsymbol{\alpha}_2, \ldots, \boldsymbol{\alpha}_i, \ldots, \boldsymbol{\alpha}_C\}$ and $\boldsymbol{\alpha}_i$ is the coefficient vector for the i^{th} class.

Hence the test sample $\boldsymbol{y}$ is represented by the linear coefficients of the training images. This coefficient vector $\boldsymbol{\alpha}$ is the sparse solution of the training images for the given test sample $\boldsymbol{y}$. It is referred to as sparse coefficient vector. Suppose if the test sample $\boldsymbol{y}$ is from the i^{th} class with n images $\boldsymbol{X}_i = \{\boldsymbol{x}_1, \boldsymbol{x}_2, \ldots, \boldsymbol{x}_n\}$ then the sparse coefficient vector is given as,

$$\boldsymbol{\alpha} = \{0, 0, \ldots, 0 | \alpha_{i,1}, \alpha_{i,2}, \ldots, \alpha_{i,n} | 0, 0, \ldots, 0\} \quad (6)$$

In the sparse solution, most of the coefficient vectors are zero, but the coefficients which are non-zero are the epochal entries. The class with which the test sample is associated has an approximate linear value and is zero otherwise [11], [13]. The sparse solution for the linear equation is achieved by L_1 norm optimization. The optimization problem can be resolved by the Greedy Pursuit Algorithms such as Basic Matching Pursuit, Basis Pursuit, Orthogonal Matching Pursuit, L_p norm regularization-based algorithms and Iterative Shrinkage Algorithms [19]. In this paper, the optimization problem is resolved by using the Basis Pursuit method. The SRC methodology can be explained as in Algorithm 2 [28], [29]. Algorithm 2.

1) The columns of the train images $\boldsymbol{X}$ are normalized to unit L_2 norm.
2) The sparse solution for normalized test sample $\boldsymbol{y}$ over train samples $\boldsymbol{X}$ is computed by L_1 norm optimization as in (7).

$$\hat{\boldsymbol{\alpha}} = argmin_{\alpha} \|\boldsymbol{\alpha}\|_1 subjected to \|\boldsymbol{y} - \boldsymbol{X}\boldsymbol{\alpha}\|_1 < \epsilon \quad (7)$$

where ϵ is a non-negative value, and in this paper $\epsilon = 0.001$.
3) The residual values are computed as,

$$\mathfrak{R}_i(y) = \|\boldsymbol{y} - \boldsymbol{X}_i\hat{\boldsymbol{\alpha}}_i\|_1 \quad (8)$$

where $\hat{\boldsymbol{\alpha}}_i$ is the coefficient vector for i^{th} class.
4) The class for $\boldsymbol{y}$ is determined as,

$$Class(\boldsymbol{y}) = argmin_i\{\mathfrak{R}_i\} \quad (9)$$

III. PROPOSED METHOD

A. THE PROPOSED kNCN-SRC METHOD

As mentioned earlier, the main objective of our proposed method *k*NCN-SRC is to enhance the recognition rate of SRC by overcoming its limitations. The principal objective of the proposed method is to classify finger vein images not only by the distances but also by spatial distribution. This is achieved by the combination of the two classification techniques *k*-NCN and SRC. The proposed *k*NCN-SRC algorithm comprises two phases.

- First phase: The NCN classification selects the k nearest train images for the given test sample $\boldsymbol{y}$.
- Second phase: The test sample $\boldsymbol{y}$ is classified by sparse representation over the k nearest train images.

The first phase of classification is achieved by the *k*-NCN classification method. As discussed earlier this classification method has two main objectives. It finds the k nearest train samples for the test sample on the basis of distance and also takes into consideration that it is spatially distributed as close as possible. These objectives can be obtained by computing the centroid distances between the images. The centroid points are computed as in (1). Subsequently, in the second phase, the selected k nearest centroid neighbors from the first stage are the train images for the classification by the SRC method.

Let $\boldsymbol{X} = \{\boldsymbol{X}_1, \boldsymbol{X}_2, \ldots, \boldsymbol{X}_p, \ldots, \boldsymbol{X}_C\}$ be the training images with C classes. Assume $\boldsymbol{X}_p = \{\boldsymbol{x}_1, \boldsymbol{x}_2, \ldots, \boldsymbol{x}_n\} \in R^{(m \times n)}$ is the n number of images in the p^{th} class. Let v be the total number of training images from all the C classes. In this paper, the training and the test images are normalized to unit L_2 norm, in order to range the features of the images from *0* to *1*. For a given test sample $\boldsymbol{y}$, the two stages of classification in the proposed *k*NCN-SRC are as follows.

In the first stage, the k nearest centroid neighbors are obtained by Algorithm 1(a). Let $\boldsymbol{Z} = \{\boldsymbol{q}_1, \boldsymbol{q}_2, \ldots, \boldsymbol{q}_k\}$ where $k \ll v$ be the selected NCN for the given test sample $\boldsymbol{y}$. In the second phase, the test sample $\boldsymbol{y}$ is represented by the linear combination as,

$$\boldsymbol{y} \approx \boldsymbol{Z}\boldsymbol{\beta} \quad (10)$$

where $\boldsymbol{\beta}$ is the sparse coefficient vector obtained by L_1 norm optimization. Assuming that the test sample $\boldsymbol{y}$ is associated with the p^{th}class then the coefficient vector is given as $\boldsymbol{\beta} = \{0, 0, \ldots, \boldsymbol{\beta}_p, 0, 0\}$.

The kNCN-SRC method can be summarized as in Algorithm 3. Algorithm 3: kNCN-SRC Algorithm

1) For the test sample $\boldsymbol{y}$, the k nearest centroid neighbors are selected from the v training images based on the steps in Algorithm 1(a). The selected k nearest centroid neighbors are given as,

$$\boldsymbol{Z} = \{\boldsymbol{q}_1, \boldsymbol{q}_2, \ldots, \boldsymbol{q}_k\} \tag{11}$$

2) The sparse solution for $\boldsymbol{y}$ over k nearest centroid neighbors ($k \ll v$) is computed by L_1 norm optimization.

$$\hat{\boldsymbol{\beta}} = argmin\|\boldsymbol{\beta}\|_1 subjected\ to \|\boldsymbol{y} - \boldsymbol{Z}\boldsymbol{\beta}\|_1 < \epsilon \tag{12}$$

where ϵ is a pixel noise level which is non-negative. In this paper $\epsilon = 0.001$.

3) The residual values are computed as,

$$\Re_p(\boldsymbol{y}) = \|\boldsymbol{y} - \boldsymbol{Z}_p\hat{\boldsymbol{\beta}}_p\|_1 \tag{13}$$

where $\hat{\boldsymbol{\beta}}_p$ is the coefficient vector for the p^{th} class.

4) The class for $\boldsymbol{y}$ is determined as the class with minimum residual value.

$$Class(\boldsymbol{y}) = \arg\min_p \{\Re_p\} \tag{14}$$

IV. COMPARISON OF *k*NCN-SRC WITH SRC, *k*NN-SRC AND TPTSR

The main principle of classification in pattern recognition is based on the closeness of the training sample to the test sample. The train samples which are near to the test sample tend to have more importance in representing the test sample than the other training samples [27]. When the proposed kNCN-SRC method was employed on the test sample, the representation results show higher sparsity than by employing the other methods such as SRC, kNN-SRC, and TPTSR. For illustration, the finger vein image from the FV-USM database is considered [31]. Figure. 1 shows the test finger vein image of the FV-USM database considered for the analysis. The sparse coefficients and the residual values for the test image for SRC, TPTSR, kNN-SRC and the proposed kNCN-SRC classification methods are shown in Figure 2. The maximum values of sparse coefficients for the test image are 0.1859, 0.0269, 0.1589, and 0.2484 when SRC, TPTSR, kNN-SRC, and kNCN-SRC as shown in Figure. 2(a), 3(a), 4(a) and 5(a) were tested, respectively. The coefficient values show that the proposed kNCN-SRC method is sparser than the other methods. It can also be observed that the class with the minimum residual value is the class of the test sample. Figures 2 (b), 3(b), 4(b) and 5(b) show the minimum residual value and the classified class for the test image considered. The minimum residual values obtained are 0.8861, 0.8939, 0.8825, and 0.2940 for SRC, TPTSR, kNN-SRC, and kNCN-SRC, respectively. The class

FIGURE 1. Test image from FV-USM database.

with the minimum residual value of *0.2940* obtained for the kNCN-SRC method is the predicted class of the test sample, which is the same as the actual class of the test sample under consideration. This is achieved for most of the test samples of the finger vein images from the other databases also.

The association of the test image with a class of the train image occurs when the non-zero entries are focused on a single train image. Hence, to estimate this distribution of the sparse coefficients, the Sparsity Concentration Index (SCI) is measured which is given as in (15) [13]. The SCI of the coefficient vector $\hat{\boldsymbol{\beta}}$ is given as,

$$SCI(\hat{\boldsymbol{\beta}}) = \frac{k \times max_i \frac{\|\delta_i(\hat{\boldsymbol{\beta}})\|_1}{\|\boldsymbol{\beta}\|_1} - 1}{k - 1} \in [0, 1] \tag{15}$$

where $\boldsymbol{\delta}_i(\hat{\boldsymbol{\beta}})$ is a vector whose non zero coefficients are from the sparse coefficient vector $\boldsymbol{\beta}$ for the i^{th} class and k is the total number of training images. The $SCI(\hat{\boldsymbol{\beta}})$ values range from 0 to 1. If $SCI(\hat{\boldsymbol{\beta}}) = 0$, the coefficients are considered to be spread all over the training images and if $SCI(\hat{\boldsymbol{\beta}}) = 1$, the coefficients are concentrated over the single class of image. The SCI values obtained for the test image shown in Figure 1 are 0.0981, 0.0001, 0.1010, and 0.9351 for the SRC, TPTSR, kNN-SRC, and kNCN-SRC classifiers respectively. It can be observed that the SCI is higher for the proposed kNCN-SRC method when compared to the other classifiers and hence it can be concluded that the concentration of the coefficients is focused more towards one

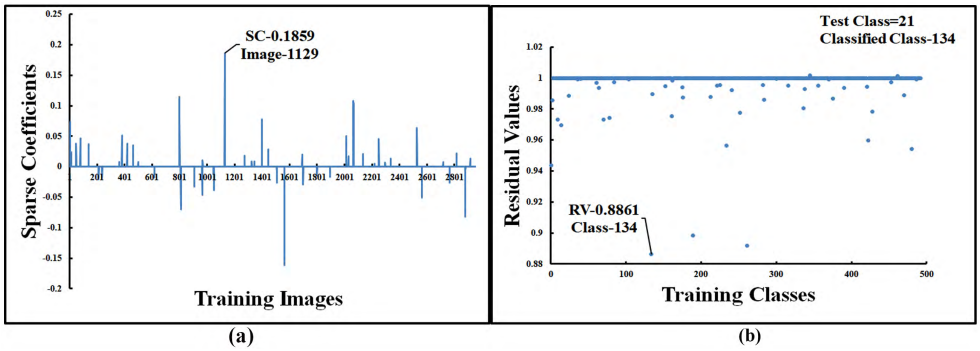

FIGURE 2. SRC. (a) Sparse coefficients. (b) Residual values representation.

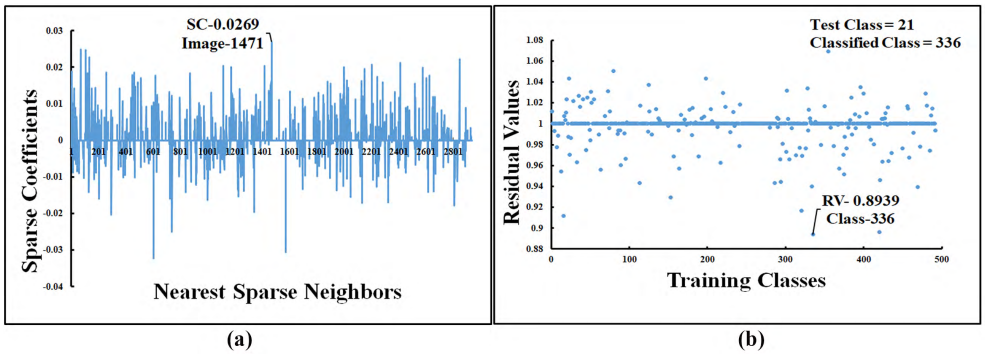

FIGURE 3. TPTSR classifier. (a) Sparse coefficients. (b) Residual values representation.

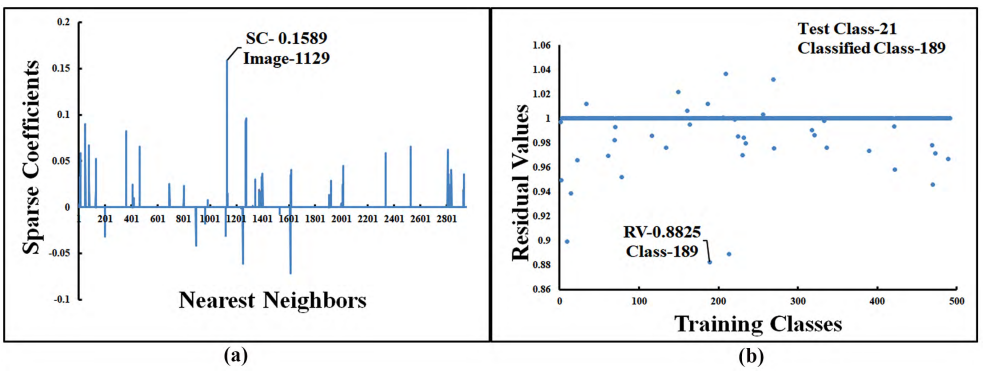

FIGURE 4. *k*NN-SRC classifier. (a) Sparse coefficients. (b) Residual values representation.

class of training images as in Figure 5 (a), and in the other classifiers it is spread over all the training images as observed in Figures 2 (a), 3 (a) and 4 (a).

V. EXPERIMENTAL RESULTS AND DISCUSSION

In this section, comparative analysis for the *k*-NN, *k*-NCN, SRC, TPTSR, CFFR, *k*NN-SRC and *k*NCN-SRC classifiers on the four public finger vein datasets are presented. In the present study, an attempt is made to prove that *k*NCN-SRC is comparatively an efficient classifier in finger vein recognition systems. The four different finger vein databases tested were Finger Vein Universiti Sains Malaysia (FV-USM) Database [31], Shandong University (SDUMLA) set up the Homologous Multi-modal Traits Database (SDUMLA-HMT) [32], the Hong Kong Polytechnic University (HKPU) Finger Image Database (finger vein) [33] and the Tsinghua University Finger Vein and Finger Dorsal Texture Database (THU-FVDT2) [34]. For comparison, the *k*-NN [35], [36], *k*-NCN [12], [24], SRC [11], CFFR [22], TPTSR [21], KCFR [23], and *k*NN-SRC [20], [37] classification methods were tested. All the experiments were run on the platform with a 2.6 GHz CPU and 4.0 GB RAM by Matlab 2015a software. The results are presented in two parts: in the first part findings of the individual classifiers are presented separately, whereas in the second part a comparative analysis of the tested classifiers is presented. In the first part, the experiments

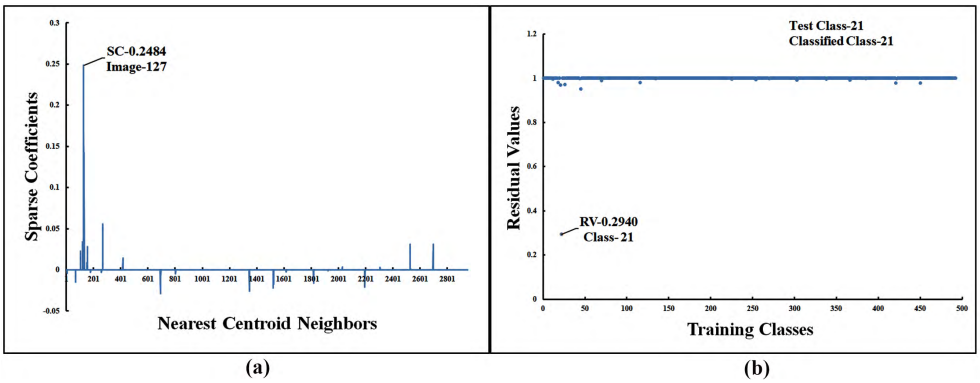

FIGURE 5. *k*NCN-SRC classifier. (a) Sparse coefficients. (b) Residual values representation.

on each classification method were conducted by selecting different parameters, whereas, in the second part, the best results obtained from the first part for the comparison of the classification techniques were considered. As the SRC classifier does not have variables, the overall results of SRC were considered directly for comparison in the second part. Similarly, results for all the four databases were analyzed using the tested classifiers.

The experimental results were evaluated by accuracy and the Kappa Coefficient *(kc)* values [38]. Accuracy is given as the ratio of the total number of correctly classified test samples to the total number of test samples. Cohen's kappa coefficient measures the inter-rater agreement between the parameters. For the experimental analysis, the inter-rater parameters are the actual class and the predicted class of the test samples. The kappa value ranges from -1 to 1. The higher the value of *kc*, the more agreement between the raters [39].

A. RESULTS FOR THE FV-USM FINGER VEIN DATASET

In this section, the experimental results obtained for the FV-USM database are discussed. For the FV-USM database, the finger vein images were collected from 123 volunteers who were the staff and students of Universiti Sains Malaysia. Each person provided four fingers: left index, left middle, right index and right middle finger with a total of 492 finger classes. The finger image was captured in two sessions with a gap of two weeks, and in each session, the finger image was captured six times. In each session a total of 2,952 ($123 \times 4 \times 6$) images were collected. Therefore, a total of *5,904* images from 492 finger classes were obtained. The spatial and depth resolution of the captured finger images were 640×480 and 256 grey levels respectively. This database is available with the extracted ROI of the finger vein images with the resolution of 300×100 pixels [31]. The images were resized to a resolution of 30×10 pixels before applying to the classification methods. The images captured at the first and second sessions were considered as the training images and the testing images, respectively. Hence, a total of 492 finger vein classes in both the train and test classes were considered. Therefore, a total of 2,952 training images and 2,952 test images were considered in the analysis. The region of interest (ROI) of the finger vein images of this database are shown in Figure 6.

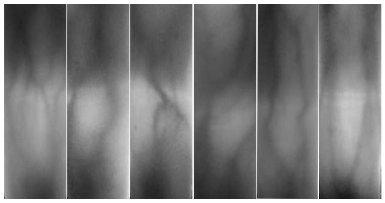

FIGURE 6. ROI of the finger vein images of the USM database.

1) PARAMETER FINDINGS FOR THE FV-USM DATABASE

The results for the parameters such as the nearest neighbor k in k-NN and k-NCN, the different number of classes (N) for CFFR, the different number of candidate classes (M) for KCFR, the different number of training images (k) for TPTSR, kNN-SRC, and kNCN-SRC classification methods are shown in Tables 1, 2, 3 and 4. From Table 1 it is observed that the best accuracy of 77.64% with $kc = 0.763$ was obtained for $k = 1$ for k-NN and k-NCN classifiers. Table 2 shows the results for CFFR classifier by considering the different number of training classes (N). It is observed that the best recognition rate of *15.48%* with $kc = 0.101$ is obtained for $N = 6$. It can be observed from Table 3 that best recognition rate of 39.43% with $kc = 0.393$ for $M = 294$ candidate classes is obtained for KCFR classifier. The TPTSR, kNN-SRC and kNCN-SRC results are shown

TABLE 1. Recognition rate of *k*-NN and *k*-NCN classifiers for FV-USM database.

k	k-NN		k-NCN	
	Accuracy (%)	kc	Accuracy (%)	kc
1	***77.64***	***0.763***	***77.64***	***0.763***
2	73.74	0.723	75.94	0.736
3	71.74	0.703	74.96	0.736
4	70.56	0.691	73.23	0.718
5	69.57	0.680	72.32	0.709

TABLE 2. Recognition rate of CFFR classifier for FV-USM database.

No. of Train Classes (N)	Accuracy (%)	kc
1	14.80	0.093
2	13.88	0.083
3	14.26	0.087
4	14.43	0.089
5	15.17	0.098
6	***15.48***	***0.101***

TABLE 3. Recognition rate of KCFR classifier for FV-USM database.

No. of Candidate Classes (M)	Accuracy (%)	kc
98	34.58	0.342
196	38.17	0.380
294	***39.43***	***0.393***

TABLE 4. Recognition rate of TPTSR, *k*NN-SRC and *k*NCN-SRC classifiers for FV-USM database.

k	TPTSR		kNN-SRC		kNCN-SRC	
	Accuracy (%)	kc	Accuracy (%)	kc	Accuracy (%)	kc
100	87.60	0.867	88.55	0.877	88.75	0.880
200	88.07	0.872	90.78	0.901	91.22	0.906
300	88.34	0.875	90.98	0.903	91.90	0.913
400	88.34	0.875	91.36	0.907	92.51	0.919
500	***88.38***	***0.876***	***91.59***	***0.910***	93.36	0.928
600	88.14	0.873	91.59	0.910	***94.41***	***0.940***

in Table 4 for the variable number of training images (k). The maximum recognition rate of 88.38% with $kc = 0.876$ for $k = 500$, 91.59% with $kc = 0.910$ for $k = 500$, and 94.41% with $kc = 0.940$ for $k = 600$ was obtained for TPTSR, kNN-SRC, and kNCN-SRC, respectively.

2) COMPARISON OF CLASSIFIERS FOR THE FV-USM DATABASE

To compare the efficiency among the tested classifiers, the best results obtained (as described in Section V-A.1) were considered. Table 5 depicts the best results obtained in each classifier along with the processing time. Table 5 also includes the results of the SRC classifier. From the results, it can be observed clearly that the highest recognition rate of 94.41% and kc=0.940 were obtained for the proposed kNCN-SRC method. In comparison with the conventional SRC, the recognition rate is improved by 3.35% for the proposed kNCN-SRC method.

TABLE 5. Comparison of the recognition results of the classifiers for FV-USM database.

Classifiers	Accuracy (%)	kc	Processing Time (s/image)
k-NN (k=1) [35], [36]	77.64	0.763	0.0005
k-NCN(k=1) [12], [24]	77.64	0.763	0.0006
SRC [11]	91.06	0.901	0.226
CFFR (N=6) [22]	15.48	0.101	2.62
KCFR (M=294) [23]	39.43	0.393	4.35
TPTSR (k=500) [21]	88.38	0.876	0.115
kNN-SRC (k=500) [20], [37]	91.59	0.910	0.132
kNCN-SRC (k=600)	***94.41***	***0.940***	***0.161***

B. RESULTS FOR THE SDUMLA-HMT FINGER VEIN DATASET

The second analysis was conducted on the SDUMLA-HMT finger vein dataset. This database is composed of images of the index, middle and ring fingers of both hands collected from each subject. This was repeated six times to obtain six replicates of finger vein images from each subject. The database was composed of $6 \times 6 \times 106 = 3,816$ images. All images were stored in 'bmp' format of 320 × 240 pixel size [32]. For this experimental analysis, the images were cropped into 300 × 100 pixel size. The images were resized to a resolution of 30 × 10 pixels before applying to the classification methods. Among the six images for each finger, three were considered as the training images and the remaining three as the test images. Hence, a total of 1,908 training images and 1,908 test images were analysed. The sample of the ROI of finger vein images of this database is shown in Figure 7.

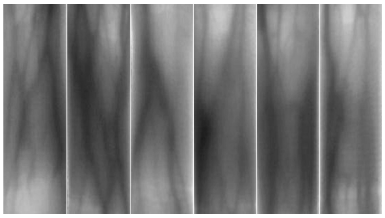

FIGURE 7. ROI of the finger vein images of the SDUMLA-HMT database.

1) PARAMETER FINDINGS FOR THE SDUMLA-HMT DATABASE

From Table 6 it is observed that the best accuracy of 50.00% with $kc = 0.497$ was obtained for $k = 1$ for k-NN and k-NCN classifiers. Tables 7, 8, and 9 show the results for CFFR, KCFR, TPTSR, kNN-SRC and kNCN-SRC classifiers, respectively. From these results, it can be observed that the maximum recognition rates obtained are 51.99% with $kc = 0.517$ for $N = 1$, 50.36% with $kc = 0.501$ for $M = 381$, 55.71% with $kc = 0.554$ for $k = 200$, 59.43% with $kc = 0.591$ for $k = 600$, and 66.56% with $kc = 0.662$ for $k = 600$, for CFFR, KCFR, TPTSR, kNN-SRC, and kNCN-SRC, respectively.

TABLE 6. Recognition rate of *k*-NN and *k*-NCN classifiers for SDUMLA-HMT database.

k	k-NN		k-NCN	
	Accuracy (%)	kc	Accuracy (%)	kc
1	***50.00***	***0.497***	***50.00***	***0.497***
2	35.27	0.350	41.87	0.416
3	29.97	0.293	39.46	0.391
4	27.93	0.277	35.90	0.356
5	23.84	0.236	34.48	0.342

2) COMPARISON OF THE CLASSIFIERS FOR THE SDUMLA-HMT DATABASE

For the comparison of the classifiers for the SDUMLA-HMT database, the best results obtained from Section V-B.1

TABLE 7. Recognition rate of CFFR classifier for SDUMLA-HMT database.

No. of Train Classes (N)	Accuracy (%)	kc
1	***51.99***	***0.517***
2	50.52	0.502
3	49.47	0.491
4	49.42	0.491
5	48.74	0.484
6	49.31	0.490

TABLE 8. Recognition rate of KCFR classifier for SDUMLA-HMT database.

No. of Candidate Classes (M)	Accuracy (%)	kc
127	48.84	0.479
254	50.26	0.492
381	***50.36***	***0.501***

TABLE 9. Recognition rate of TPTSR, *k*NN-SRC and *k*NCN-SRC classifiers for SDUMLA-HMT database.

k	TPTSR		kNN-SRC		kNCN-SRC	
	Accuracy (%)	kc	Accuracy (%)	kc	Accuracy (%)	kc
100	55.03	0.547	57.12	0.568	57.28	0.569
200	***55.71***	***0.554***	57.91	0.576	59.32	0.590
300	55.13	0.548	58.28	0.579	60.11	0.598
400	54.87	0.545	58.80	0.585	62.15	0.618
500	54.45	0.541	59.01	0.587	64.67	0.643
600	53.93	0.536	***59.43***	***0.591***	***66.56***	***0.662***

TABLE 10. Comparison of the recognition results of the classifiers for SDUMLA-HMT database.

Classifiers	Accuracy (%)	kc	Processing Time (s/image)
k-NN (k=1) [35], [36]	50.00	0.497	0.00043
k-NCN(k=1) [12], [24]	50.00	0.497	0.00045
SRC [11]	57.49	0.570	0.175
CFFR (N=1) [22]	51.99	0.517	0.890
KCFR (M=381) [23]	50.36	0.501	2.21
TPTSR (k=200) [21]	55.71	0.554	0.052
kNN-SRC (k=600) [20], [37]	59.43	0.591	0.167
kNCN-SRC (k=600)	***66.56***	***0.662***	***0.154***

were considered. Tables 10 depicts the best results obtained in each classifier including the SRC classifier. The highest recognition rate of 66.56% and kc = 0.662 was obtained for the proposed kNCN-SRC method. The recognition rate is increased by 9.07% in comparison with the conventional SRC.

C. RESULTS FOR THE HKPU FINGER VEIN DATABASE

The results of the experimental analysis for HKPU finger vein database are discussed in this section. This database consists of images of finger vein and finger surface texture from male and female volunteers. In this paper, the finger vein images were considered for the experimental analysis. The database had 6,264 images obtained from 156 subjects. The finger images were taken in two different sessions. The second session took place at an interval 11 months after the first session. Six image samples of the index and middle fingers of both hands were taken from each subject. Therefore, each subject provided 24 images in one session. All images were in bmp format of 580 × 380 pixel size [33]. For the analysis, a total of 2,520 finger vein images were considered, from which 1,260 were from the first session and 1,260 were from the second session. All the images were cropped manually to 300 × 100 pixel size. The images were resized to a resolution of 30 × 10 pixels before applying to the classification methods. The first session images were considered to be the training images and the second session were considered to be the test images. The sample of the ROI of finger vein images of this database is shown in Figure 8.

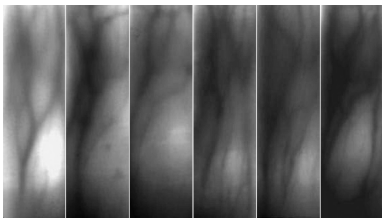

FIGURE 8. ROI of the finger vein images of the HKPU database.

1) PARAMETER FINDINGS FOR THE HKPU DATABASE

From Table 11 it is observed that the best accuracy of 27.77% with kc = 0.255 was obtained for k = 1 for k-NN and k-NCN classifiers. Tables 12, 13 and 14 show the results for CFFR, KCFR, TPTSR, kNN-SRC and kNCN-SRC classifiers, respectively. From the results, it can be observed that the maximum recognition rate obtained was 66.66% with kc = 0.653 for N = 4, 51.58% with kc = 0.513 for M = 42, 45.79% with kc = 0.424 for k = 300, 51.03% with k = 0.475 for k = 500, and 69.52% with kc = 0.659 for k = 600 for CFFR, KCFR, TPTSR, kNN-SRC, and kNCN-SRC, respectively.

TABLE 11. Recognition rate of *k*-NN and *k*-NCN classifiers for HKPU database.

k	k-NN		k-NCN	
	Accuracy (%)	kc	Accuracy (%)	kc
1	***27.77***	***0.255***	***27.77***	***0.255***
2	23.09	0.213	24.28	0.222
3	18.65	0.171	23.17	0.213
4	17.77	0.164	22.30	0.205
5	17.61	0.162	21.34	0.196

TABLE 12. Recognition rate of CFFR classifier for HKPU database.

No. of Train Classes (N)	Accuracy (%)	kc
1	58.41	0.562
2	63.41	0.618
3	64.68	0.631
4	***66.66***	***0.653***
5	64.12	0.625
6	64.60	0.630

2) COMPARISON OF THE CLASSIFIERS FOR THE HKPU DATABASE

For the comparison of the classifiers for the HKPU database, the best results obtained from Section V-C.1 were considered.

TABLE 13. Recognition rate of KCFR classifier for HKPU database.

No. of Candidate Classes (M)	Accuracy (%)	kc
42	***51.58***	***0.513***
84	48.73	0.487
126	48.49	0.483

TABLE 14. Recognition rate of TPTSR, *k*NN-SRC and *k*NCN-SRC classifiers for HKPU database.

k	TPTSR		*k*NN-SRC		*k*NCN-SRC	
	Accuracy (%)	kc	Accuracy (%)	kc	Accuracy (%)	kc
100	44.04	0.407	48.25	0.448	49.84	0.464
200	44.84	0.416	50.31	0.468	54.68	0.511
300	***45.79***	***0.424***	50.63	0.471	57.76	0.538
400	45.39	0.421	50.71	0.473	60.31	0.566
500	45.15	0.418	***51.03***	***0.475***	65.47	0.618
600	45.39	0.421	50.79	0.473	***69.52***	***0.659***

TABLE 15. Comparison of the recognition results of the classifiers for HKPU database.

Classifiers	Accuracy (%)	kc	Processing Time (s/image)
k-NN (*k*=1) [35], [36]	27.77	0.255	0.00028
k-NCN(*k*=1) [12], [24]	27.77	0.255	0.00033
SRC [11]	49.29	0.459	0.235
CFFR (*N*=4) [22]	66.66	0.653	0.295
KCFR (*M*=42) [23]	51.58	0.513	0.955
TPTSR (*k*=300) [21]	45.79	0.424	0.039
*k*NN-SRC (*k*=500) [20], [37]	51.03	0.475	0.118
*k*NCN-SRC (*k*=600)	***69.52***	***0.659***	***0.143***

Table 15 depicts the best results obtained in each classifier along with the SRC classifier. The highest recognition rate of 69.52% and kc = 0.659 was obtained for the proposed *k*NCN-SRC method. An increase in recognition rate of 20.23% is obtained for the proposed method in comparison with the conventional SRC.

D. RESULTS FOR THE THU-FVDT2 FINGER VEIN DATABASE

The THU-FVDT2 database provides the ROI of the finger vein images. The images were recorded in two different sessions at an interval of three days to one week from 610 subjects. The images from the first session are considered as the train and the images from the other session as the test. The resolution of the captured images is 720 × 576 pixels with 96 dpi. The ROI of the images are normalized to 200 × 100 pixels [34]. For our analysis, the ROI images are resized to 20 × 10 pixels before considering it for the classification process. The sample finger vein images of this database are shown in Figure 9.

1) PARAMETER FINDINGS FOR THE THU-FVDT2 DATABASE

From Table 16 it is observed that the best accuracy of 69.67% with kc = 0.696 was obtained for k = 1 for *k*-NN and *k*-NCN classifiers. Tables 17, 18 and 19 show the results for CFFR, KCFR, TPTSR, *k*NN-SRC and *k*NCN-SRC classifiers, respectively. From the results, it can be observed that the maximum recognition rate obtained was 22.29% with

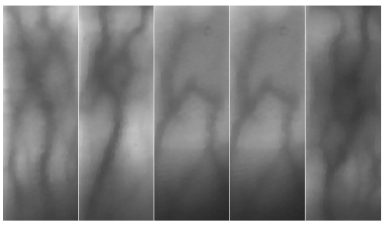

FIGURE 9. ROI of the finger vein images of THU-FVDT2 database.

TABLE 16. Recognition rate of *k*-NN and *k*-NCN classifiers for THUFVDT2 database.

k	*k*-NN		k-NCN	
	Accuracy (%)	kc	Accuracy (%)	kc
1	***69.67***	***0.696***	***69.67***	***0.696***
2	5.57	0.055	36.39	0.363
3	5.73	0.057	27.04	0.270
4	4.75	0.047	20.65	0.206
5	3.11	0.031	15.73	0.157

TABLE 17. Recognition rate of CFFR classifier for THU-FVDT2 database.

No. of Train Classes (N)	Accuracy (%)	kc
1	3.27	0.031
2	7.70	0.075
3	12.95	0.128
4	17.54	0.174
5	20.54	0.202
6	***22.29***	***0.222***

TABLE 18. Recognition rate of KCFR classifier for THU-FVDT2 database.

No. of Candidate Classes (M)	Accuracy (%)	kc
122	24.42	0.244
244	25.57	0.255
366	***26.72***	***0.267***

TABLE 19. Recognition rate of TPTSR, *k*NN-SRC and *k*NCN-SRC classifiers for THU-FVDT2 database.

k	TPTSR		*k*NN-SRC		*k*NCN-SRC	
	Accuracy (%)	kc	Accuracy (%)	kc	Accuracy (%)	kc
100	91.96	0.919	94.91	0.949	95.24	0.952
200	94.59	0.945	***95.73***	***0.957***	96.39	0.963
300	***95.24***	***0.952***	95.51	0.951	***96.88***	**0.968**

$kc = 0.222$ for $N = 6$, 26.72% with $kc = 0.267$ for $M = 366$, 95.24% with $kc = 0.952$ for $k = 300$, 95.73% $kc = 0.957$ for $k = 200$, and 96.88% with $kc = 0.968$ for $k = 300$ for CFFR, KCFR, TPTSR, *k*NN-SRC, and *k*NCN-SRC, respectively.

2) COMPARISON OF THE CLASSIFIERS FOR THE THU-FVDT2 DATABASE

In order to compare the tested classifiers for the THU-FVDT2 database, the best results obtained from Section V-D.1 were considered. Table 20 depicts the best results obtained in each classifier along with the SRC classifier. The highest recognition rate of 96.88% with

TABLE 20. Comparison of the recognition results of the classifiers for THU-FVDT2 database.

Classifiers	Accuracy (%)	*kc*	Processing Time (s/image)
k-NN (*k*=1) [35], [36]	69.67	0.696	0.0021
k-NCN(*k*=1) [12], [24]	69.67	0.696	0.0021
SRC [11]	96.07	0.960	0.052
CFFR (*N*=6) [22]	22.29	0.222	0.075
KCFR (*M*=366) [23]	26.72	0.267	0.525
TPTSR (*k*=300) [21]	95.24	0.952	0.046
*k*NN-SRC (*k*=200) [20], [37]	95.73	0.957	0.130
*k*NCN-SRC (*k*=300)	***96.88***	***0.968***	***0.050***

$kc = 0.968$ for $k = 300$ was obtained for the proposed *k*NCN-SRC method. An increase 0.81% of recognition rate is obtained for the proposed method in comparison with the conventional SRC.

E. PROCESSING TIME

To analyse the processing time comparatively, the time for the best recognition rate for each classifier is taken into consideration. Tables 5, 10, 15 and 20 depict the computational time of each algorithm for all the tested databases. Among all the tested algorithms, the *k*-NN and *k*-NCN algorithms based on Euclidean distances were computationally efficient. The algorithm TPTSR is based on L_2 norm which is computationally efficient. The CFFR algorithm is also based on L_2 norm, but it is computationally inefficient for large databases. The KCFR algorithm based on kernel feature space representation is also computationally inefficient for large databases. The algorithms SRC, *k*NN-SRC and the *k*NCN-SRC were all implemented based on L_1 norm; however, SRC was found to be computationally time-consuming and *k*NN-SRC showed improved computational efficiency, whereas *k*NCN-SRC displayed most computational efficiency compared to both SRC and *k*NN-SRC. The main reason for the highest efficiency of *k*NCN-SRC could be attributed to the reduction of the train samples by considering the nearest centroid neighbors for the SRC computation in the second stage. By the overall comparison, it can be concluded that the proposed *k*NCN-SRC method is computationally faster than the SRC algorithms and is nearly equal to *k*NN-SRC.

VI. CONCLUSION

In this paper, a new classification method called *k*NCN-SRC algorithm for efficient recognition of finger vein images is proposed. The main objective of this algorithm is to determine the nearest centroid neighbors for the SRC computation, thereby reducing the training images during SRC classification. The *k*NCN-SRC algorithm considers the distance factor as well as the spatial distribution factor during the classification of images. The recognition rate of the proposed *k*NCN-SRC method was found to be most efficient compared to the other tested algorithms. The efficiency of the *k*NCN-SRC method could be due to the consideration of the spatial distribution factor. Additionally, the processing time is fast due to the reduction of the training samples for SRC classification in the second stage. Compared with the other tested algorithms such as SRC, TPTSR, CFFR, KCFR, and *k*NN-SRC, the proposed *k*NCN-SRC algorithm performs more efficiently with a higher recognition rate as demonstrated in the present experiments.

REFERENCES

[1] M. Xue and Q. Sun, "Vasculature development in embryos and its regulatory mechanisms," *Chin. J. Comparative Med.*, vol. 13, no. 1, pp. 45–49, Jan. 2003.
[2] L. Yang, G. Yang, X. Xi, X. Meng, C. Zhang, and Y. Yin, "Tri-branch vein structure assisted finger vein recognition," *IEEE Access*, vol. 5, pp. 21020–21028, Jul. 2017.
[3] H. Liu, L. Yang, G. Yang, and Y. Yin, "Discriminative binary descriptor for finger vein recognition," *IEEE Access*, vol. 6, pp. 5795–5804, Dec. 2018.
[4] H. Qin, X. He, X. Yao, and H. Li, "Finger-vein verification based on the curvature in radon space," *Expert Sys. Appl.*, vol. 82, pp. 151–161, Oct. 2017.
[5] J. Yang, Y. Shi, and G. Jia, "Finger-vein image matching based on adaptive curve transformation," *Pattern Recognit.*, vol. 66, pp. 34–43, Jun. 2017.
[6] R. B. JosephP and D. Ezhilmaran, "A smart computing algorithm for finger vein matching with affine invariant features using fuzzy image retrieval," *Procedia Comput. Sci.*, vol. 125, pp. 172–178, Jan. 2018.
[7] T. Liu, J. Xie, W. Yan, P. Li, and H. Lu, "Finger-vein pattern restoration with direction-variance-boundary constraint search," *Eng. Appl. Artif. Intell.*, vol. 46, pp. 131–139, Nov. 2015.
[8] L. Yang, G. Yang, Y. Yin, and X. Xi, "Finger vein recognition with anatomy structure analysis," *IEEE Trans. Circuits Syst. Video Technol.*, vol. 28, no. 8, pp. 1892–1905, Mar. 2018.
[9] P. Gupta and P. Gupta, "An accurate finger vein based verification system," *Digit. Signal Process.*, vol. 38, pp. 43–52, Mar. 2015.
[10] H. C. Lee, B. J. Kang, E. C. Lee, and K. R. Kang, "Finger vein recognition using weighted local binary pattern code based on a support vector machine," *J. Zhejiang Uni. Sci. C*, vol. 11, no. 7, pp. 514–524, Jul. 2010.
[11] Y. Xin, Z. Liu, H. Zhang, and H. Zhang, "Finger vein verification system based on sparse representation," *Appl. Opt.*, vol. 51, no. 25, pp. 6252–6258, Jul. 2012.
[12] B. A. Rosdi, H. Jaafar, and D. A. Ramli, "Finger vein identification using fuzzy-based k-nearest centroid neighbor classifier," in *Proc. AIP Conf.*, Feb. 2015, vol. 1643, no. 1, pp. 649–654.
[13] Z. Fan, D. Zhang, X. Wang, Q. Zhu, and Y. Wang, "Virtual dictionary based kernel sparse representation for face recognition," *Pattern. Recognit.*, vol. 76, pp. 1–13, Apr. 2018.
[14] M. Rajabi, S. Ghofrani, and A. Ayatollahi, "A new iris segmentation method based on sparse representation," *J. Adv. Comput. Res.*, vol. 8, no. 1, pp. 89–105, 2017.
[15] G. Shao, Y. Wu, A. Yong, X. Liu, and T. Guo, "Fingerprint compression based on sparse representation," *IEEE Trans. Image Process.*, vol. 23, no. 2, pp. 489–501, Feb. 2014.
[16] I. Rida, S. Al-Maadeed, A. Mahmood, A. Bouridane, and S. Bakshi, "Palmprint identification using an ensemble of sparse representations," *IEEE Access*, vol. 6, pp. 3241–3248, Jan. 2018.
[17] Z. Yuting, P. Gang, K. Jia, M. Lu, Y. Wang, and Z. Wu, "Accelerometer-based gait recognition by sparse representation of signature points with clusters," *IEEE Trans. Cybern.*, vol. 45, no. 9, pp. 1864–1875, Sep. 2015.
[18] S. S. Chen, D. L. Donoho, and M. A. Saunders, "Atomic decomposition by basis pursuit," *SIAM Rev.*, vol. 43, no. 1, pp. 129–159, 2001.
[19] J. Yang, Y. Peng, W. Xu, and Q. Dai, "Ways to sparse representation: An overview," *Sci. China F, Inf. Sci.*, vol. 52, no. 4, pp. 695–703, Apr. 2009.
[20] N. Zhang and J. Yang, "K nearest neighbor based local sparse representation classifier," in *Proc. Chin. Conf. Pattern Recognit. (CCPR)*, Oct. 2010, pp. 1–5.
[21] Y. Xu, D. Zhang, J. Yang, and J.-Y. Yang, "A two-phase test sample sparse representation method for use with face recognition," *IEEE Trans. Circuits Syst. Video Technol.*, vol. 21, no. 9, pp. 1255–1262, Sep. 2011.
[22] Y. Xu, Q. Zhu, Z. Fan, D. Zhang, J. Mi, and Z. Lai, "Using the idea of the sparse representation to perform coarse-to-fine face recognition," *Inf. Sci.*, vol. 238, pp. 48–138, Jul. 2013.
[23] S. Zeng, X. Yang, and J. Gou, "Using kernel sparse representation to perform coarse-to-fine recognition of face images," *Optik*, vol. 140, pp. 528–535, Jul. 2017.

[24] B. B. Chaudhuri, "A new definition of neighborhood of a point in multi-dimensional space," *Pattern Recognit. Lett.*, vol. 17, no. 1, pp. 11–17, Jan. 1996.
[25] J. S. Sanchez, F. Pla, and F. J. Ferri, "On the use of neighbourhood-based non-parametric classifiers," *Pattern. Recognit. Lett.*, vol. 18, no. 11, pp. 1179–1186, Nov. 1997.
[26] J. Gou, Z. Yi, L. Du, and T. Xiong, "A local mean-based K-nearest centroid neighbor classifier," *Comput. J.*, vol. 55, no. 9, pp. 1058–1071, Jan. 2012.
[27] J. Gou, Z. Yi, L. Du, and T. Xiong, "Weighted K-nearest centroid neighbor classification," *J. Comput. Inf. Syst.*, vol. 8, no. 2, pp. 851–860, Feb. 2012.
[28] L. Zhang, M. Yang, and X. Feng, "Sparse representation or collaborative representation: Which helps face recognition?" in *Proc. IEEE Int. Conf. Comput. Vis. (ICCV)*, Nov. 2011, pp. 471–478.
[29] Z. Fan, M. Ni, Q. Zhu, and E. Liu, "Weighted sparse representation for face recognition," *Neurocomputing*, vol. 151, pp. 304–309, Mar. 2015.
[30] Y. Cong, J. Yuan, and J. Liu, "Sparse reconstruction cost for abnormal event detection," in *Proc. IEEE Conf. Comp. Vis. Pattern Recognit. (CVPR)*, Jun. 2011, pp. 3449–3456.
[31] M. S. M. Asaari, S. A. Suandi, and B. A. Rosdi, "Fusion of band limited phase only correlation and width centroid contour distance for finger based biometrics," *Expert Syst. Appl.*, vol. 41, no. 7, pp. 3367–3382, Jun. 2014.
[32] Y. Yin, L. Liu, and X. Sun, "SDUMLA-HMT: A multimodal biometric database," in *Proc. 6th Chin. Conf. Biometric Recognit. Biometric Recognit.*, Dec. 2011, pp. 260–268.
[33] A. Kumar and Y. Zhou, "Human identification using finger images," *IEEE Trans. Image Process.*, vol. 21, no. 4, pp. 2228–2244, Apr. 2012.
[34] W. Yang, F. Zhou, and Q. Liao, "Feature-level fusion of finger veins and finger dorsal texture for personal authentication based on orientation selection," *IEICE Trans. Inf. Syst.*, vol. 97, no. 5, pp. 1371–1373, May 2014.
[35] B. W. Silverman and M. C. Jones, "E. Fix and J. L. Hodges (1951): An important contribution to nonparametric discriminant analysis and density estimation: Commentary on Fix and Hodges (1951)," *Int. Stat. Rev./Revue Internationale Statistique*, vol. 57, no. 3, pp. 233–238, Dec. 1989.
[36] S. Damavandinejadmonfared, A. K. Mobarakeh, S. A. Suandi, and B. A. Rosdi, "Evaluate and determine the most appropriate method to identify finger vein," *Procedia Eng.*, vol. 41, pp. 516–521, Jan. 2012.
[37] S. Shazeeda and B. A. Rosdi, "Finger vein identification based on the fusion of nearest neighbor and sparse representation based classifiers," *Indian J. Sci. Technol.*, vol. 9, no. 48, pp. 1–7, Dec. 2016.
[38] Y. Qian, M. Ye, and J. Zhou, "Hyperspectral image classification based on structured sparse logistic regression and three-dimensional wavelet texture features," *IEEE Trans. Geosci. Remote Sens.*, vol. 51, no. 4, pp. 2276–2291, Apr. 2013.
[39] J. Cohen, "Weighted kappa: Nominal scale agreement provision for scaled disagreement or partial credit," *Psychol. Bull.*, vol. 70, no. 4, pp. 213–220, Oct. 1968.

SHAZEEDA SHAZEEDA received the B.E. degree in electronic and communication engineering from the Bapuji Institute of Engineering and Technology, India, in 2001, the M.E. degree in digital communications and networking from the University B.D.T. College of Engineering, India, in 2006, and the Ph.D. degree in image processing from Universiti Sains Malaysia, Pulau Pinang, Malaysia, in 2018. She was an Assistant Professor with the S.J.M. Institute of Technology, India. Her research interest includes the application of pattern recognition in finger vein biometrics.

BAKHTIAR AFFENDI ROSDI received the B.Eng., M.Eng., and D.Eng. degrees in electrical and electronic engineering from the Tokyo Institute of Technology, Tokyo, Japan, in 1999, 2004, and 2007, respectively. He is currently an Associate Professor with the School of Electrical and Electronic Engineering, Universiti Sains Malaysia, Pulau Pinang, Malaysia. His research interests include the application of pattern recognition in biometrics and bioinformatics applications. He has served as a reviewer for a few international conferences and journals including *Sensors*, *Information Sciences*, *Image and Vision Computing*, and *IET Biometrics*.